Vibrational excitation of methylamine by electron impact in the 4.5–30 eV energy range

F. Motte-Tollet, M.-J. Hubin-Franskin, and J. E. Collin

Citation: The Journal of Chemical Physics **97**, 7314 (1992); doi: 10.1063/1.463503
View online: http://dx.doi.org/10.1063/1.463503
View Table of Contents: http://scitation.aip.org/content/aip/journal/jcp/97/10?ver=pdfcov
Published by the AIP Publishing

Vibrational excitation of methylamine by electron impact in the 4.5–30 eV energy range

F. Motte-Tollet, M.-J. Hubin-Franskin,[a] and J. E. Collin
Laboratoire de Spectroscopie d'Electrons diffusés, Université de Liège, Institut de Chimie-Bâtiment B6, Sart Tilman par 4000 Liège 1, Belgium

(Received 2 June 1992; accepted 31 July 1992)

Vibrational excitation of gaseous methylamine induced by 4.5–30 eV energy electrons has been investigated by the electron energy loss spectroscopy. The ratios of the differential cross sections for excitation of the vibrational modes and for elastic scattering measured as a function of the electron kinetic energies show that at 15 and 30 eV, the vibrational excitation occurs mainly through a direct mechanism. The absolute vibrationally elastic and inelastic differential cross sections have been measured at these impact energies. The cross sections for the inelastic scattering are strongly dependent on the vibrational mode which is excited.

I. INTRODUCTION

Vibrational excitation of molecules in their electronic ground state by low energy electrons has been studied extensively. At these energies, the scattering process is often dominated by a shape resonance.[1] Direct vibrational transitions can also take place through the dependence of the electron–molecule interaction on the vibrational coordinates of the molecule (i.e., by a direct nonresonant process).[2,3] Moreover, at electron impact energies near threshold, vibrational excitation can proceed through a virtual state.[4] Such a state has been found experimentally for polar and for nonpolar molecules.[5–7]

The direct vibrational excitation by electron impact has been largely investigated in diatomic molecules.[8–14] In homonuclear molecules, excitation of electric-dipole-forbidden vibrations has been evidenced[15] and is due mainly to the contributions of the quadrupole and polarization interaction terms to the vibrational cross sections.[15,16] However, for infrared-active heteronuclear molecules, the contribution of the long-range dipole interaction to the vibrational excitation is expected to be the largest, at least at low scattering angles.[17,18] Some studies have also dealt with the nonresonant vibrational excitation in linear and some nonlinear triatomic molecules.[19–22] However, less is known about the vibrational excitation in larger molecules, characterized by a high number of vibrational modes.[23–25]

The measurement of the direct vibrational cross sections is of fundamental interest. Indeed, the behavior of the vibrational cross section vs the scattering angle or the impact energy can be related to the different electron–molecule interaction terms (dipole, quadrupole, polarization,...) and then to the nature of the target molecule potential.[18] For example, the differential cross sections of electric-dipole-allowed vibrational modes are characterized by a strong forward scattering that evidences the long-range electric-dipole electron–molecule interaction.[18,26] Such behavior is found for the deformation and asymmetric stretching vibrational modes in CO_2 (Refs. 27 and 28). The vibrational excitation processes are also of great importance to understand the atmospheres of the earth and other planets as well as the composition and physical properties of interstellar matter. Other fields of applications are also found in gaseous laser media, in gaseous discharges, or in electron impact-induced chemical reactions on surfaces.

The present work is devoted to the study of the polar molecule methylamine which has been included in the chemical models of the atmospheres of Uranus, Saturn, and Jupiter[29–31] and which is a typical molecule in the research field of the surface physical chemistry.[32] We have investigated the elastic and vibrational scattering by the gaseous molecule by the electron energy loss method at impact energies outside the 7.5 eV and the higher energy ($\geqslant$8.3 eV) resonances which have been reported in a previous work.[33] The absolute elastic differential cross sections have been determined between 8° and 115° for 15 and 30 eV impact energies. The vibrational excitation spectra and the absolute vibrationally inelastic differential cross sections have been measured at these electron energies in the 8°–75° angular range. The behaviors of the vibrational cross sections have allowed us to discuss the electron–molecule interaction potential and especially to define the contribution of the dipole force to the vibrational excitation.

II. EXPERIMENT

The apparatus used for the present measurements is a Vacuum Generator SEELS 400, modified for work on gaseous target. It has been described previously.[34] A 150° hemispherical-sector electrostatic electron monochromator fitted with a three-element lens produces an energy-selected electron beam of the required impact energy. The incident electron beam current is typically of $5–10\times10^{-10}$ A as monitored by a Faraday cup mounted recently on the spectrometer and described in detail elsewhere.[35] The gas is introduced using a 1 mm diameter hypodermic needle. The scattered electrons are energy analyzed in an analyzer of the same type as the monochromator rotatable from 0° to +120° around the forward direction and detected by an

[a]Maître de Recherches F.N.R.S.

 0021-9606/92/227314-09$006.00

electron multiplier of the channeltron type. The residual pressure is about 1×10^{-8} Torr and rises to 1×10^{-5} Torr when the gas is on.

The apparatus has been operated in two different modes, i.e., the energy loss mode at fixed electron impact energy and angle and the angular differential cross section mode for a defined energy loss and at fixed impact energy.

All measurements have been made at constant pass energy. The resolution of the whole spectrometer has been set between 23 and 40 meV, according to the experimental conditions. The calibration of the energy loss scale has been performed using the elastic peak as the zero of the scale.

The collision volume angular dependence has been checked with nitrogen by measuring the 15 and 30 eV elastic differential cross sections in the angular range of interest for this study and by comparing them to the absolute values of Srivastava *et al.*[36] renormalized to the latest measurements of the He absolute elastic differential cross section.[37] This set of absolute values has been chosen because the measurements were performed at the same scattering angles than ours. It is in very good agreement within the experimental errors with the more recent absolute values of Shyn and Carignan.[38]

The relative elastic differential cross sections have been normalized to the absolute scale at a scattering angle of 20° by means of a relative flow technique with nitrogen as calibration standard.[39] The experimental setup will be described in detail in a further paper.[35] Briefly, the intensity of electrons elastically scattered from N_2 has been measured and immediately followed by the measurements of the scattered electron intensity from CH_3NH_2 under the same experimental conditions. The mass flow rates and then the head pressures have been adjusted to reproduce as closely as possible the same flux distribution from the hypodermic needle of both gases.[40,41] In the present measurements, 1.2 Torr N_2 gas pressure behind the hypodermic needle and 0.7 Torr CH_3NH_2 head pressure have been chosen. These back pressure values have kept the vacuum chamber pressure on the 10^{-6} Torr range throughout the experiment. Then the measured differential cross sections have been converted into absolute cross sections by use of the formula

$$\frac{\mathrm{DCS}(CH_3NH_2,\theta)}{\mathrm{DCS}(N_2,\theta)}=[\mathrm{Ne}(CH_3NH_2)/\mathrm{Ne}(N_2)]\times[m(N_2)/m(CH_3NH_2)]^{1/2}\times[\mathrm{Nb}(N_2)/\mathrm{Nb}(CH_3NH_2)],$$

where $\mathrm{Ne}(CH_3NH_2)$ and $\mathrm{Ne}(N_2)$ are the experimentally measured intensities (as integrated peak counts) of elastically scattered electrons, $m(N_2)$ and $m(CH_3NH_2)$ are molecular weights, $\mathrm{Nb}(N_2)$ and $\mathrm{Nb}(CH_3NH_2)$ are mass flow rates of the two gases into the scattering chamber as measured by mass flow meters, and $\mathrm{DCS}(N_2,\theta)$ is the N_2 absolute elastic differential cross section renormalized to the latest measurements of the He absolute elastic differential cross section.[36,37] The background contribution to the elastic-scattered intensity (both the direct electron beam contribution and scattering by the background gas) has been estimated by directing the gas flow to either the hypodermic needle or the side leak.[35,36] It has been found that at 15 and 30 eV impact energies, the background contribution was about 2% for scattering angles of 20° or larger. At smaller scattering angles, the direct beam contribution may become more important. However, we have checked that this contribution was negligible in comparison with other sources of errors for the 8°–20° angular range.

From the energy loss spectra recorded at various angles, the ratio of the peak areas of the vibrational and the elastic scattering excitations has been determined as a function of the scattering angle. As these ratios are equal (to a good approximation) to the corresponding cross section ratios, the absolute elastic differential cross sections have been used together with these intensity ratios to obtain the absolute angular distributions after the vibrational excitation of CH_3NH_2. The contribution to the vibrational intensity by the elastic peak has been estimated by drawing a visually smooth profile of the vibrational-excitation feature. The vibrational peaks which overlap in the spectra have been unfolded by using an approximate visual deconvolution with Gaussian feature shapes.

The gas sample has been the commercial one from Union Carbide with a purity better than 99%. It has been used without further purification.

III. THE METHYLAMINE CHARACTERISTICS

The methylamine molecule presents one symmetry plane which contains the carbon–nitrogen axis and is bisecting the $\widehat{HNH}$ angle and thus belongs to the Cs symmetry group. It has 15 normal vibrational modes which all are both infrared and Raman active. Nine modes are of the A' type, whereas the others have A'' symmetry. The corresponding wave numbers (in cm^{-1}), energies (in meV), symmetries, natures, and relative intensities in infrared and Raman gaseous spectroscopies are presented in Table I.[42–44] To our knowledge, the absolute values for the variations of the electric dipole moment and of the polarizability have not been determined.

Methylamine has a permanent dipole moment of 1.23 D and a polarizability of 4 $Å^3$.[45,46] As far as we know, no data on the value of the electric quadrupole moment of the molecule have been published.

IV. RESULTS

We first report the vibrational energy loss spectra ($\Delta v=1$ and 2) of methylamine recorded at 15 and 30 eV impact energies for various scattering angles. The spectra have been limited to the energy loss range of 0–1 eV, corresponding to the excitation of the fundamental modes and of some harmonics and combinations.

Second, the ratios of the vibrationally elastic and inelastic scattering peaks are expressed as a function of the electron impact energy.

TABLE I. Symmetries, natures of modes, wave numbers (in cm^{-1}), energies (in meV), and relative intensities in infrared and Raman spectroscopies for the fundamental vibrations of the methylamine molecule (Refs. 42–44).[a]

Symmetry		Nature of the mode	Wave number (cm^{-1})	Energy (meV)	Relative intensity	
					IR	Raman
A'	ν_1	NH_2 stretching	3361	417	W	VS
	ν_2	CH_3 stretching	2961	367	VS	VS
	ν_3	CH_3 stretching	2820	350	VS	S
	ν_4	NH_2 scissoring	1623	201	S	
	ν_5	CH_3 deformation	1473	183	S	M
	ν_6	CH_3 deformation	1430	177	M	
	ν_7	CH_3 rocking	1130	140	M	
	ν_8	CN stretching	1044	129	S	S
	ν_9	NH_2 wagging	780	97	VS	W
A''	ν_{10}	NH_2 stretching	3427	425	W	W
	ν_{11}	CH_3 stretching	2985	370	VS	
	ν_{12}	CH_3 deformation	1485	184		
	ν_{13}	NH_2 twisting	...	...		
	ν_{14}	CH_3 rocking	1195	148		
	ν_{15}	Torsion	268	33		

[a]VS—very strong, S—strong, M—medium, and W—weak.

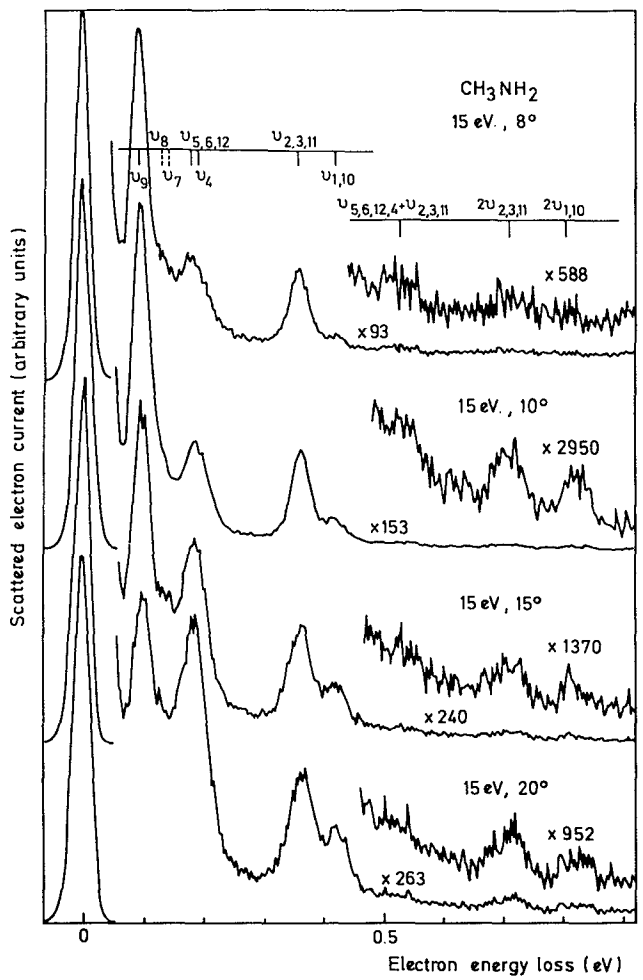

FIG. 1. Vibrational energy loss spectra recorded at 15 eV impact energy for 8°, 10°, 15°, and 20° scattering angles.

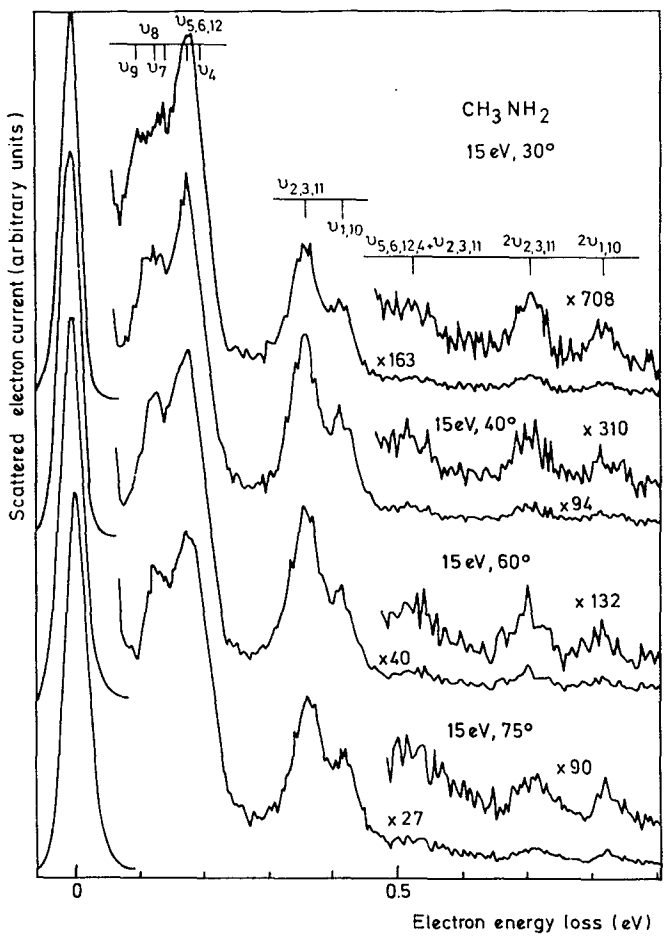

FIG. 2. Vibrational energy loss spectra recorded at 15 eV impact energy for 30°, 40°, 60°, and 75° scattering angles.

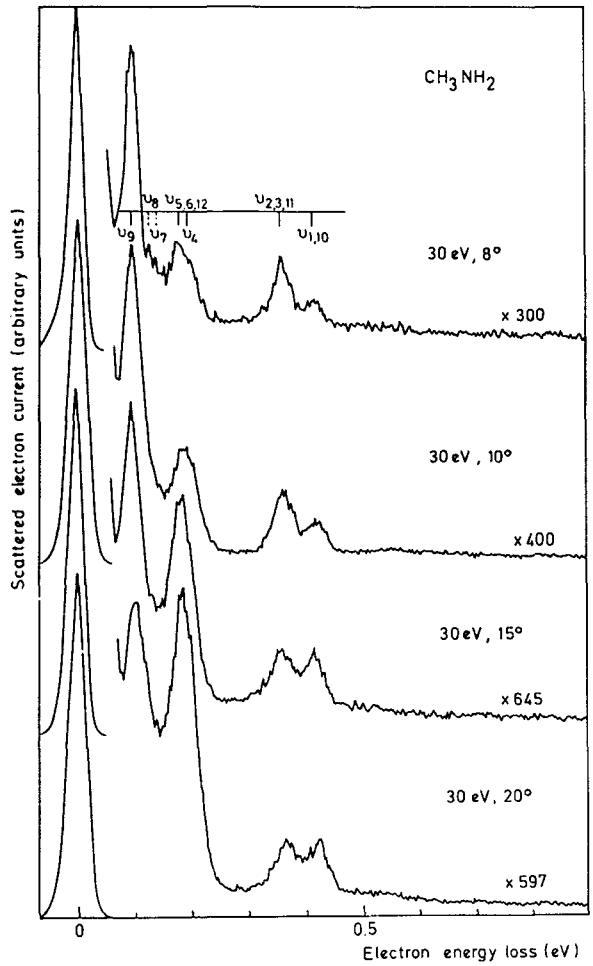

FIG. 3. Vibrational energy loss spectra recorded at 30 eV impact energy for 8°, 10°, 15°, and 20° scattering angles.

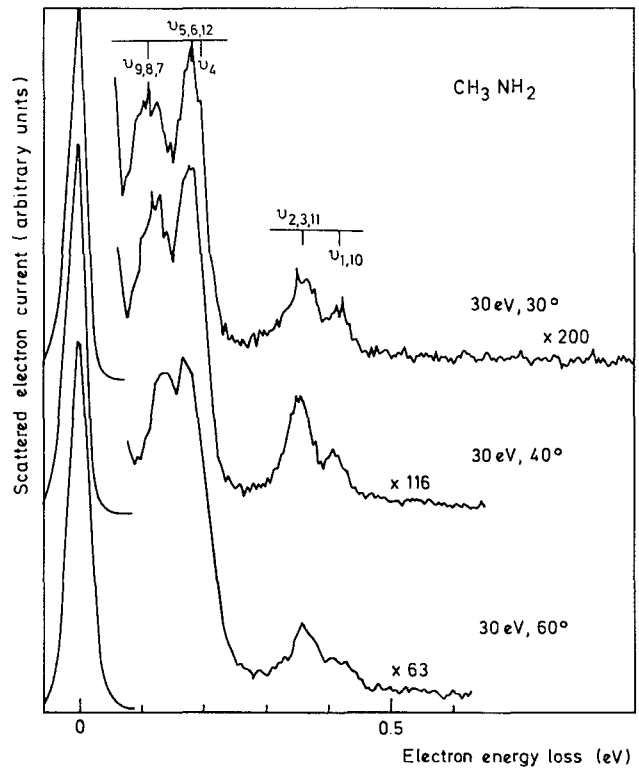

FIG. 4. Vibrational energy loss spectra recorded at 30 eV impact energy for 30°, 40°, and 60° scattering angles.

Finally, the absolute elastic and vibrational angular differential cross sections obtained at 15 and 30 eV impact energies are presented.

A. Electron energy loss spectra

The 15 and 30 eV vibrational excitation spectra are presented in Figs. 1–4. At low scattering angles, they are composed of the elastic peak and of five bands which are related to the excitation of the various normal modes. The first inelastic band located at 97 meV corresponds to the excitation of the amino-wagging vibrational mode ν_9. At 132 meV appears a much lower intensity band related to the CN stretching vibration (ν_8) and the symmetric CH_3 rocking vibration (ν_7). These modes cannot be resolved within the experimental resolution and are labeled $\nu_{8,7}$ (this notation will be used throughout the description of the spectra and the discussion). The CH_3 and NH_2 deformation modes ($\nu_{5,6,12}$ and ν_4) are observed at 182 meV energy loss. The excitation of the stretching vibrations of the methyl group corresponds to the 362.5 meV band which will be labeled $\nu_{2,3,11}$. The NH_2 stretching modes ($\nu_{1,10}$) manifest themselves at the high energy side of the $\nu_{2,3,11}$ band by an incompletely resolved peak located at 418

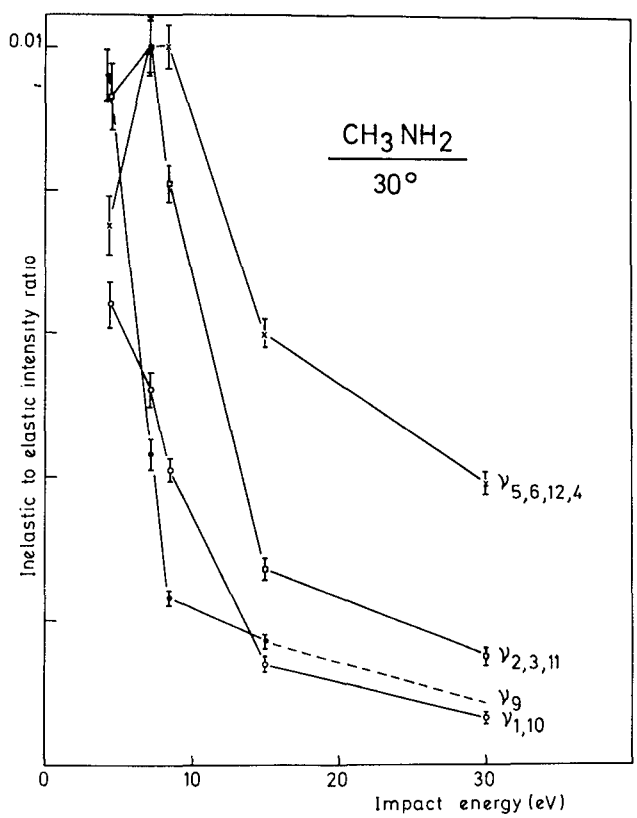

FIG. 5. Ratios of the vibrationally elastic and inelastic differential cross sections at 4.5, 7.2, 8.5, 15, and 30 eV for a 30° scattering angle.

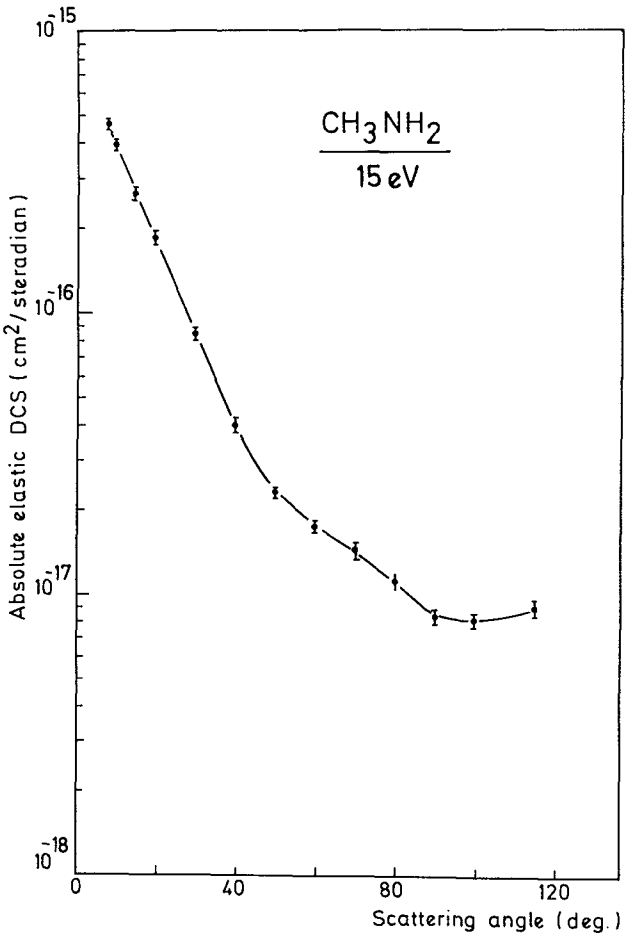

FIG. 6. Absolute elastic differential cross section vs the scattering angle at 15 eV.

meV. Possibly the torsion vibrational mode ν_{15} ($\Delta E=33$ meV) might contribute to broaden the "elastic" peak and cannot be resolved. Finally, at 15 eV impact energy, additional bands are observed at higher energy losses, i.e., at 526, 712, and 820 meV. They correspond to the excitation of the combinations between the $\nu_{5,6,12,4}$ and the $\nu_{2,3,11}$ groups, of the harmonics of the CH_3 stretching modes $2\nu_{2,3,11}$ and of those of the NH_2 stretching modes $2\nu_{1,10}$, respectively. In particular, the spectra recorded at 8°, i.e., when the electric dipole interaction between the electron and the molecule is the most important, agree qualitatively with those obtained by infrared spectroscopy (Table I).

For larger scattering angles, the overall shape of the spectra changes. On the one hand, a drastic diminution in relative intensity is observed for the ν_9 band, which becomes no longer resolvable from the $\nu_{8,7}$ group of modes at 30°. On the other hand, a strong increase of the relative intensity of the $\nu_{8,7}$ and the $\nu_{5,6,12,4}$ bands manifests itself and the band related to the excitation of the CH_3 and NH_2 deformation modes ($\nu_{5,6,12,4}$) dominates the spectra at high scattering angles ($\geqslant 30°$).

B. Ratios of the vibrationally elastic and inelastic differential cross sections as a function of the electron impact energy

The ratios of the vibrationally elastic and inelastic scattering peaks have been derived at 30° on basis of the peak area from the electron energy loss spectra recorded at 4.5, 7.2, 8.5, 15, and 30 eV. They are displayed in Fig. 5 as a function of the electron impact energy.

The CH_3 and NH_2 deformation modes ($\nu_{5,6,12,4}$) ratio presents a broad maximum in the 7–9 eV region, while the CH_3 stretching modes ($\nu_{2,3,11}$) ratio exhibits a maximum centered at about 7.2 eV, but less broad. The occurrence of maxima in these curves shows evidence that the vibrational excitation of these groups of modes proceeds in this energy range mainly through an indirect mechanism by way of the shape resonances at 7.5 eV and at higher impact energy ($\geqslant 8.3$ eV) as related in detail in our previous work.[33] These resonances seem to have a minor effect on the NH_2 stretching modes ($\nu_{1,10}$), the associated ratio being quite less enhanced.

The ν_9 mode ratio increases very strongly below 8.5 eV, but does not exhibit any structure. That confirms that the amino-wagging deformation mode is not influenced by these shape resonances and that it is excited mainly through a direct mechanism, even at low electron impact energy.

Finally, the intensity ratios reported in Fig. 5 seem to behave smoothly between 15 and 30 eV impact energies. This hypothesis is supported by the fact that the values of the ratios at 15 eV are lower than at 8.5 eV and that those at 30 eV are even lower than at 15 eV. Then the vibrational excitation takes place very probably through a direct mechanism at 15 and 30 eV.

C. Absolute elastic and vibrational differential cross sections at 15 and 30 eV impact energies

The absolute elastic differential cross sections at 15 and 30 eV are displayed in Figs. 6 and 7, respectively, and are tabulated in Table II. The statistical uncertainties in the relative behavior of the cross section are indicated by error bars in the figures. The error of the normalization procedure by the relative flow technique is estimated to be $\pm 27\%$. This represents the square root of the quadratic sum of a $\pm 24\%$ error in the ratio measurements (which is analyzed in Table III) and of a $\pm 13\%$ error in the N_2 absolute elastic differential cross section of Srivastava *et al.*[36] It should be noted that the largest contribution to the $\pm 24\%$ error arises from the measurement of the CH_3NH_2 flow rate, the flow through the hypodermic needle being difficult to establish within the short time of the experiment (about 20 min). Both cross sections are forward peaking in the 8°–40° angular range with absolute values of 9.3×10^{-16} and of 4.8×10^{-16} (cm^2/sr) at 30 eV, 8° and 15 eV, 8°, respectively. They decrease less rapidly between 40° and 90°.

At 15 eV impact energy, the measurements have been made up to 115°. There is a slight enhancement of the cross section above 100°.

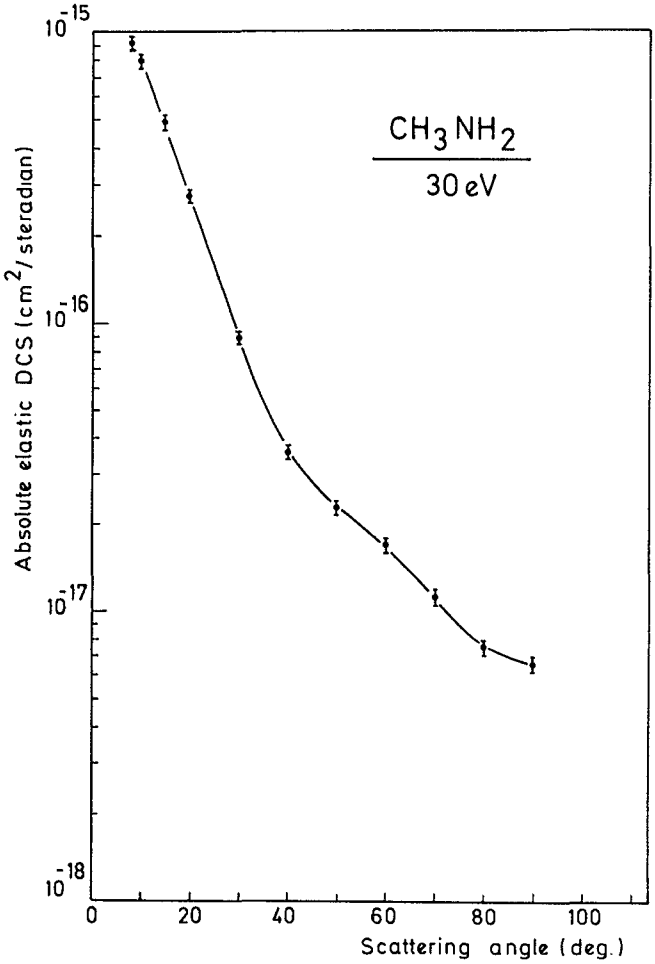

FIG. 7. Absolute elastic differential cross section vs the scattering angle at 30 eV.

The 15 and 30 eV differential cross sections of the various groups of modes are presented in Figs. 8 and 9 and are reported in tabular form in Tables IV and V, respectively. The errors in the relative angular dependence of the vibrational cross sections are shown by error bars in the figures, while the uncertainty on the absolute values is estimated to be ±30%. The value of this latter error increases for the ν_9 and $\nu_{5,6,12,4}$ groups of modes, for which the contribution of the elastic peak becomes more important.

TABLE II. Absolute elastic differential cross sections of CH_3NH_2 at 15 and 30 eV impact energies as a function of the scattering angle. Units are 10^{-16} cm²/sr.

θ (degrees)	15 eV	30 eV
8	4.8	9.3
10	4.1	8.2
15	2.8	5.0
20	1.9	2.8
30	0.87	0.92
40	0.41	0.37
50	0.24	0.23
60	0.18	0.18
70	0.15	0.12
80	0.12	0.078
90	0.084	0.067
100	0.083	···
115	0.090	···

TABLE III. Various sources of errors that contribute to the total error in the measurement of the ratio $DCS(CH_3NH_2,\theta)/DCS(N_2,\theta)$.

1.	Estimated error in the ratio of flow rates $Nb(N_2)/Nb(CH_3NH_2)$	±15%
2.	Estimated error in the ratio $Ne(CH_3NH_2)/Ne(N_2)$.	±6%
3.	Estimated error due to the change in the incident electron beam current	±3%
Total		±24%

At 15 eV energy impact and for low scattering angles (8°–30°), the differential cross sections of the various groups of modes exhibit different behaviors. It should be noted that the ν_9 cross section has a value of 3.0×10^{-18} (cm²/sr) at 8° and decreases very rapidly as a function of the scattering angle. The largest variation of the cross section at low angles after ν_9 is for $\nu_{2,3,11}$, for which a value of 1.4×10^{-18} (cm²/sr) has been measured at 8°. The varia-

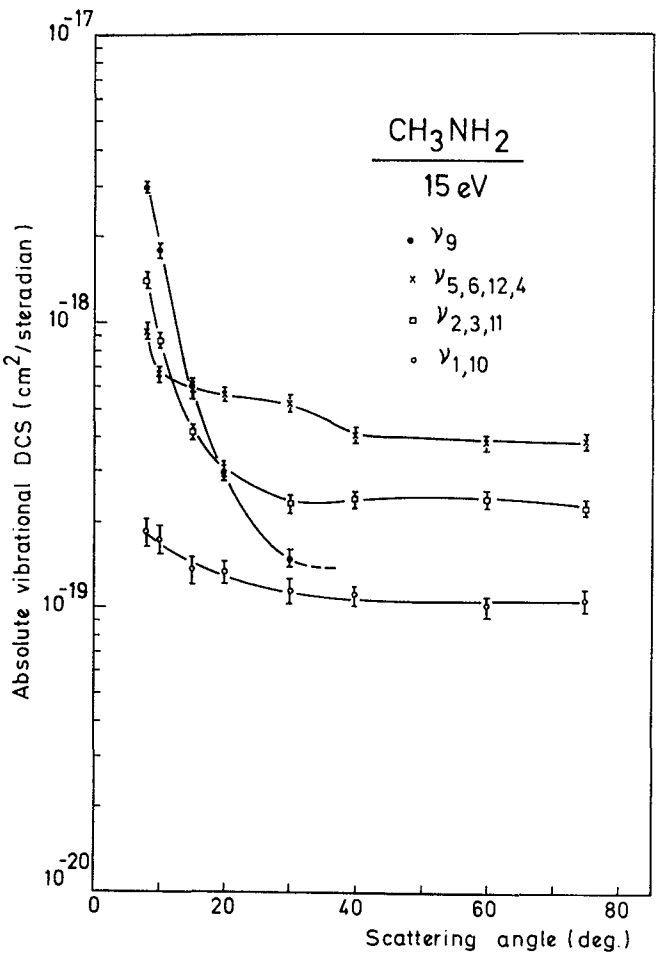

FIG. 8. Absolute vibrational differential cross section vs the scattering angle at 15 eV.

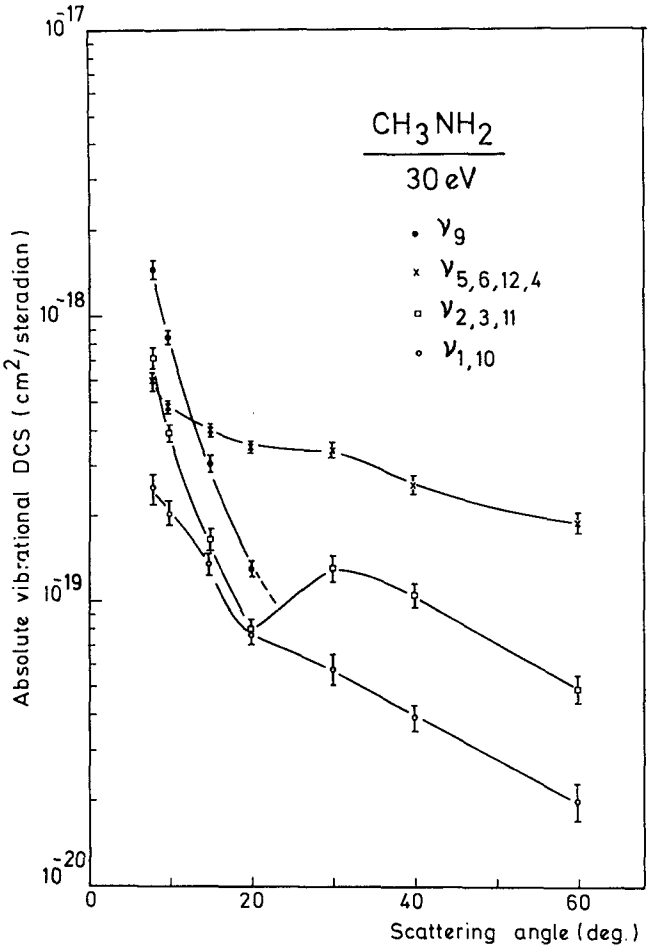

FIG. 9. Absolute vibrational differential cross section vs the scattering angle at 30 eV.

tion of the $\nu_{5,6,12,4}$ and $\nu_{1,10}$ cross sections is less important for the same angular range. The $\nu_{1,10}$ cross section is only of 1.9×10^{-19} (cm^2/sr) at 8°, i.e., an order of magnitude smaller than for the other modes. For higher scattering angles (30°–75°), the $\nu_{2,3,11}$ and $\nu_{1,10}$ cross sections both present an isotropic behavior (Fig. 8). The cross section of the CH_3 and NH_2 deformation modes ($\nu_{5,6,12,4}$) seems to exhibit a smooth maximum at about 30° and then shows an isotropic behavior. No information can be obtained for the

TABLE IV. Absolute differential cross sections of the various groups of vibrational modes of CH_3NH_2 at 15 eV impact energy as a function of the scattering angle. Units are 10^{-19} cm^2/sr.

θ (degrees)	ν_9	$\nu_{5,6,12,4}$	$\nu_{2,3,11}$	$\nu_{1,10}$
8	30	9.5	14	1.9
10	19	6.7	8.8	1.8
15	6.1	6.0	4.2	1.4
20	3.1	5.7	3.1	1.4
30	1.5	5.3	2.4	1.2
40	···	4.1	2.5	1.1
60	···	3.8	2.4	1.0
75	···	3.8	2.3	1.1

TABLE V. Absolute differential cross sections of the various groups of vibrational modes of CH_3NH_2 at 30 eV impact energy as a function of the scattering angle. Units are 10^{-19} cm^2/sr.

θ (degrees)	ν_9	$\nu_{5,6,12,4}$	$\nu_{2,3,11}$	$\nu_{1,10}$
8	15	6.1	7.3	2.6
10	8.5	4.9	3.9	2.1
15	3.1	4.1	1.7	1.4
20	1.3	3.6	0.82	0.77
30	···	3.5	1.3	0.58
40	···	2.6	1.1	0.39
60	···	1.9	0.49	0.20

NH_2 wagging deformation mode (ν_9) above 30°, where the related band is no longer resolvable from the other bands due to its low intensity.

The 30 eV angular differential cross sections in the angular range of 8°–20° present qualitatively the same behaviors than at 15 eV (Figs. 8 and 9). The ν_9 and $\nu_{2,3,11}$ cross sections are both peaking at low angles with values of 1.5×10^{-18} and 7.3×10^{-19} (cm^2/sr), respectively, at 8°. The $\nu_{1,10}$ cross section at 8° is of 2.6×10^{-19} (cm^2/sr), i.e., a little larger than at 15 eV, contrary to the other vibrational cross sections. Between 20° and 60°, the cross sections present different behaviors according to the various groups of modes excited (Fig. 9). Indeed, the cross section corresponding to the CH_3 stretching modes ($\nu_{2,3,11}$) shows a pronounced maximum ~30°–40°, while that relating to the NH_2 stretching vibrations ($\nu_{1,10}$) and to the $\nu_{5,6,12,4}$ group of modes decreases smoothly in this angular range.

V. DISCUSSION

The shapes of the angular differential cross sections at 15 and 30 eV for the various groups of modes in CH_3NH_2 will be discussed in terms of the electron–molecule interactions inducing the vibrational excitation. Moreover, a comparison will be made with other molecules including dipolar ones.

A. The shape of the differential cross sections at 15 eV

1. The ν_9 mode

The differential cross section of the amino-wagging deformation mode (ν_9) exhibits the largest variation in the 8°–30° angular range and is very strongly forward peaked (Fig. 8). Such a behavior is similar to that observed for the bending (010) and asymmetric (001) infrared-active vibrational modes in CO_2.[19,26–28] In ammonia, the cross section of the "umbrella" deformation mode (ν_2) also shows a strong decrease in the 10°–30° angular range.[23] It should be noted that this normal mode is associated with the largest variation of the dipole moment during the vibration[47] and that the corresponding ν_9 mode in methylamine is also strongly infrared active (Table I).

In CO_2, the strong forward scattering observed in the cross sections of the infrared-active modes is known to be related to the long-range dipole interaction term between the electron and the molecule.[27,48,49] In the analogy to that

molecule, we suggest that the ν_9 vibrational mode in methylamine is mainly excited through the electric dipole potential scattering, at least for low detection angles.[18,49]

2. The $\nu_{2,3,11}$ group of modes

This group of modes corresponds to the CH_3 stretching vibrational modes ν_2, ν_3, and ν_{11}, which are not resolved within our experimental resolution. ν_2 and ν_3 are symmetric vibrations, while ν_{11} is the asymmetric stretching vibrational mode of the CH_3 group. The ν_2 and ν_3 components are very strong infrared and Raman active, while the ν_{11} component is strongly infrared active, but has not been observed in the Raman spectrum (Table I).

The differential cross section of the CH_3 stretching modes decreases very rapidly between 8° and 30° and presents the largest variation after that of ν_9 (Fig. 8). Since all the components are very strongly infrared active (Table I), we propose that the excitation of the CH_3 stretching modes at low scattering angles is dominated mainly by the long-range dipole interaction, just as it was suggested above for the ν_9 mode.

When the scattering angle rises, the shape of the cross section changes drastically and becomes isotropic in the 30°–75° angular range (Fig. 8). This behavior has been found for the vibrational cross sections in several molecules at the same impact energy. We shall discuss some examples below. The cross section relating to the optically forbidden mode in nitrogen presents an isotropic shape in the 40°–80° angular range.[12] For such a nonpolar homonuclear diatomic molecule, it has been evidenced that the vibrational excitation occurs mainly through the electric quadrupole and the polarization interaction terms, often called "shorter-ranged terms".[15,16,50] Trajmar *et al.*[51] have measured the angular differential cross section of the $\nu_{1,3}$ group of modes in water at 15 eV impact energy. It should be noted that the ν_1 and ν_3 modes are both infrared and Raman active. They found an isotropic shape for the related cross section from 30° to about 70°. Itikawa[52] has calculated the angular cross section of that group of modes at the same energy using the Born theory and taking into account not only the long-range dipole interaction term, but also the quadrupole and polarization interaction terms, which contribute mainly to the larger-angle scattering.[18,49] Measurements of differential cross sections have also been reported for the $\nu_{1,3}$ and $\nu_{2,4}$ groups of modes in CH_4.[53–55] The ν_3 and ν_4 components are infrared active, but all four are Raman active. The cross section of the $\nu_{1,3}$ group of modes exhibits a nearly isotropic behavior in a wide angular range, while that relating to the $\nu_{2,4}$ composite has two broad features, a minimum in the region of 60°–80° and a maximum between 110° and 130°. Moreover, vibrational excitation has been investigated recently in ethane.[25] At 15 eV, the differential cross section relating to the group of mainly deformation modes (which are infrared and/or Raman active) also behaves isotropically between 40° and 100°. The comparison of the angular differential cross section of the $\nu_{2,3,11}$ group of modes with those reported in other molecules suggests that the excitation of the CH_3 stretching modes takes place mainly through the quadrupole and polarization interaction potentials at high scattering angles ($\geqslant$30°).

3. The $\nu_{1,10}$ group of modes

The ν_1 vibrational mode is the symmetric stretching of the NH_2 group and is weakly infrared and strongly Raman active (Table I). The ν_{10} vibrational mode is related to the NH_2 asymmetric stretching vibration and is weakly infrared and Raman active. The two components are not resolved within our experiment.

The differential cross section of the $\nu_{1,10}$ group of modes is displayed in Fig. 8. It diminishes slowly in the 8°–30° angular range and becomes isotropic above 30°. The decrease of the cross section at low scattering angles is much less important than that evidenced for the ν_9 and the $\nu_{2,3,11}$ vibrational modes. The two composites ν_1 and ν_{10} being weakly infrared active, this can be due to a "less important" long-range dipole interaction between the electron and the molecule. However, above 30°, the shape of the $\nu_{1,10}$ cross section is similar to that of the $\nu_{2,3,11}$ one. This may be due to the strong contribution of the shorter-ranged interaction terms (quadrupole, polarization,...) to the larger-angle scattering relative to that of the long-range dipole one.

4. The $\nu_{5,6,12,4}$ group of modes

The CH_3 and NH_2 deformation modes cross section becomes isotropic only for scattering angle larger than 40° (Fig. 8). Then, the relative magnitudes of the various interaction terms would be different from that observed in the $\nu_{2,3,11}$ and $\nu_{1,10}$ cross sections for the higher angular range.

B. The shape of the differential cross sections at 30 eV

1. The ν_9 mode

The angular differential cross section of the ν_9 mode measured at 30 eV impact energy presents a very forward peaked behavior, as at 15 eV energy (Figs. 8 and 9).

2. The $\nu_{2,3,11}$ group of modes

The differential cross section of the CH_3 stretching modes ($\nu_{2,3,11}$) diminishes very rapidly between 8° and 20°, as observed at lower impact energy (Figs. 8 and 9). However, at higher scattering angles, it exhibits a maximum located around 30°–40°. This might be due to the increase with the kinetic energy of the incident electron of the electric quadrupole interaction term.[15,52,56] Such a maximum has also been reported in the vibrational cross section for the CO molecule at 50, 75, and 100 eV impact energies[57] as well as in the cross section of the $v=1$ vibrational level in nitrogen at 75 eV.[11]

3. The $\nu_{1,10}$ and $\nu_{5,6,12,4}$ groups of modes

At the impact energy of 30 eV, the cross section of the NH_2 stretching modes diminishes smoothly between 8° and 60°. Its shape is different from that measured at 15 eV,

especially for the 30°–60° angular range. For that Raman-active and weakly infrared-active group of modes, the cross section is no more isotropic at 30 eV for scattering angles $\geqslant 30°$. In addition, it is a little bit more forward peaking than at 15 eV at low angles. Again that indicates the strong dependence of the relative contributions of the interaction terms on the impact energy. However, it should be noted that the behavior of the $\nu_{5,6,12,4}$ differential cross section at 30 eV is quite similar to that observed at 15 eV.

VI. CONCLUSIONS

Excitation of the vibrational normal modes of methylamine has been studied by low and intermediate energy electron impact. Electron energy loss spectra have been recorded at 4.5, 7.2, 8.5, 15, and 30 eV impact energies for various scattering angles.

The ratios of the differential cross sections for the vibrationally elastic and inelastic scattering as a function of the impact energy have shown that at 15 and 30 eV, the vibrational excitation occurs mainly through a direct mechanism.

We have reported the absolute angular elastic and vibrational differential cross sections for 15 and 30 eV kinetic energies.

The analysis of the results indicates that the behavior of the vibrational differential cross sections of such a highly polar molecule is strongly dependent on the vibrational mode which is excited and on the impact energy.

ACKNOWLEDGMENTS

We are grateful to the I.R.S.I.A and to the Fonds National de la Recherche Scientifique of Belgium for research grant (FMT) and position (MJHF). We also acknowledge the Patrimoine of the University of Liège, the Fonds National de la Recherche Scientifique, and the Service de la Programmation de la Politique Scientifique (A.R.C.) for financial support. We wish also to express our gratitude to J. Heinesch for his highly valuable technical assistance.

[1] G. J. Schulz, Rev. Mod. Phys. **45**, 423 (1973).
[2] G. J. Schulz, *Principles of Laser Plasmas*, edited by G. Bekefi (Wiley-Interscience, New York, 1976).
[3] K. Takayanagi, in *Electron–Molecule Collisions*, edited by I. Shimamura and K. Takayanagi (Plenum, New York, 1984).
[4] L. Dubé and A. Herzenberg, Phys. Rev. Lett. **38**, 820 (1977).
[5] K. Rohr and F. Linder, J. Phys. B **9**, 2521 (1976).
[6] W. Sohn, K. Jung, and H. Ehrhardt, J. Phys. B **16**, 891 (1983).
[7] M. Rädle, G. Knoth, K. Jung, and H. Ehrhardt, J. Phys. B **22**, 1455 (1989).
[8] R. W. Crompton, D. K. Gibson, and A. G. Robertson, Phys. Rev. A **2**, 1386 (1970).
[9] S. Trajmar, D. G. Truhlar, J. K. Rice, and A. Kuppermann, J. Chem. Phys. **52**, 4516 (1970).
[10] D. G. Truhlar, S. Trajmar, and W. Williams, J. Chem. Phys. **57**, 3250 (1972).
[11] D. G. Truhlar, M. A. Brandt, S. K. Srivastava, S. Trajmar, and A. Chutjian, J. Chem. Phys. **66**, 655 (1977).
[12] H. Tanaka, T. Yamamoto, and T. Okada, J. Phys. B **14**, 2081 (1981).
[13] H. Nishimura, A. Danjo, and H. Sugahara, J. Phys. Soc. Jpn. **54**, 1757 (1985).
[14] W. Sohn, K. H. Kochem, K. Jung, H. Ehrhardt, and E. S. Chang, J. Phys. B **18**, 2049 (1985).
[15] A. Skerbele, M. A. Dillon, and E. N. Lassettre, J. Chem. Phys. **49**, 3543 (1968).
[16] K. Takayanagi, J. Phys. Soc. Jpn. **20**, 562 (1965).
[17] K. Takayanagi, Suppl. Prog. Theor. Phys. **40**, 216 (1967).
[18] Y. Itikawa, J. Phys. Soc. Jpn. **28**, 1062 (1970).
[19] D. F. Register, H. Nishimura, and S. Trajmar, J. Phys. B **13**, 1651 (1980).
[20] K. H. Kochem, W. Sohn, N. Hebel, K. Jung, and H. Ehrhardt, J. Phys. B **18**, 4455 (1985).
[21] W. Sohn, K. H. Kochem, K. M. Scheuerlein, K. Jung, and H. Ehrhardt, J. Phys. B **20**, 3217 (1987).
[22] M. Furlan, M.-J. Hubin-Franskin, J. Delwiche, and J. E. Collin, J. Chem. Phys. **95**, 1671 (1991).
[23] M. Furlan, M.-J. Hubin-Franskin, J. Delwiche, and J. E. Collin, J. Chem. Phys. **92**, 213 (1990).
[24] K. H. Kochem, W. Sohn, K. Jung, H. Ehrhardt, and E. S. Chang, J. Phys. B **18**, 1253 (1985).
[25] L. Boesten, H. Tanaka, M. Kubo, H. Sato, M. Kimura, M. A. Dillon, and D. Spence, J. Phys. B **23**, 1905 (1990).
[26] A. Skerbele, M. A. Dillon, and E. N. Lassettre, J. Chem. Phys. **49**, 5042 (1968).
[27] A. Andrick, D. Danner, and H. Ehrhardt, Phys. Lett. A **29**, 346 (1969).
[28] H. Ehrhardt, K. Jung, K. H. Kochem, and W. Sohn, Lect. Notes Chem. **35**, 32 (1984).
[29] B. Fegley and R. G. Prinn, Astrophys. J. **299**, 1067 (1985).
[30] E. Lellouch and J. L. Destombes, Astron. Astrophys. **152**, 405 (1985).
[31] B. Fegley and R. G. Prinn, Astrophys. J. **307**, 852 (1986).
[32] A. G. Baca, M. A. Schulz, and D. A. Shirley, J. Chem. Phys. **83**, 6001 (1985).
[33] F. Motte-Tollet, M.-J. Hubin-Franskin, and J. E. Collin, J. Chem. Phys. **93**, 7843 (1990).
[34] M. Furlan, M.-J. Hubin-Franskin, J. Delwiche, D. Roy, and J. E. Collin, J. Chem. Phys. **82**, 1797 (1985).
[35] F. Motte-Tollet, M.-J. Hubin-Franskin, M. Furlan, J. Delwiche, and J. E. Collin (to be published).
[36] S. K. Srivastava, A. Chutjian, and S. Trajmar, J. Chem. Phys. **64**, 1340 (1976).
[37] D. F. Register, S. Trajmar, and S. K. Srivastava, Phys. Rev. A **21**, 1134 (1980).
[38] T. W. Shyn and G. R. Carignan, Phys. Rev. A **22**, 923 (1980).
[39] S. K. Srivastava, A. Chutjian, and S. Trajmar, J. Chem. Phys. **63**, 2659 (1975).
[40] S. Trajmar and D. F. Register, in *Electron–Molecule Collisions*, edited by I. Shimamura and K. Takayanagi (Plenum, New York, 1984).
[41] J. C. Nickel, P. W. Zetner, G. Shen, and S. Trajmar, J. Phys. E **22**, 730 (1989).
[42] J. S. Kirby-Smith and L. G. Bonner, J. Chem. Phys. **7**, 880 (1939).
[43] A. P. Gray and R. C. Lord, J. Chem. Phys. **26**, 690 (1957).
[44] T. Shimanouchi, *Tables of Molecular Vibrational Frequencies* (U.S. GPO, Washington, DC, 1972).
[45] K. Takagi and T. Kojima, J. Phys. Soc. Jpn. **30**, 1145 (1971).
[46] A. A. Radzig and B. M. Smirnov, *Reference Data on Atoms, Molecules, and Ions* (Springer, Berlin, 1985).
[47] D. C. Mc Kean and P. Schatz, J. Chem. Phys. **24**, 316 (1985).
[48] Y. Itikawa, Phys. Rev. A **3**, 831 (1971).
[49] Th. Antoni, K. Jung, H. Ehrhardt, and E. S. Chang, J. Phys. B **19**, 1377 (1986).
[50] Y. Itikawa, Phys. Rep. **46**, 117 (1978).
[51] S. Trajmar, W. Williams, and A. Kuppermann, J. Chem. Phys. **58**, 2521 (1973).
[52] Y. Itikawa, J. Phys. Soc. Jpn. **36**, 1127 (1974).
[53] H. Tanaka, M. Kubo, N. Onodera, and A. Suzuki, J. Phys. B **16**, 2861 (1983).
[54] P. J. Curry, W. R. Newell, and A. C. H. Smith, J. Phys. B **18**, 2303 (1985).
[55] T. W. Shyn, J. Phys. B **24**, 5169 (1991).
[56] E. N. Lassettre, A. Skerbele, and V. D. Meyer, J. Chem. Phys. **45**, 3214 (1966).
[57] A. Chutjian and H. Tanaka, J. Phys. B **13**, 1901 (1980).